ELSEVIER

Thin Solid Films 357 (1999) 119–124

thin solid films

www.elsevier.com/locate/tsf

Electrodeposition of Sn, Se, SnSe and the material properties of SnSe films

B. Subramanian[c], T. Mahalingam[a], C. Sanjeeviraja[a,*], M. Jayachandran[b], Mary Juliana Chockalingam[b]

[a]*Department of Physics, Alagappa University, Karaikudi 630003, India*
[b]*Central Electrochemical Research Institute, Karaikudi 630006, India*
[c]*Jayaram College of Engineering and Technology, Karattampatti 621014, India*

Received 1 December 1998; received in revised form 19 August 1999; accepted 19 August 1999

Abstract

A detailed account of the electrochemistry involved in the deposition of Sn, Se and SnSe films is presented. The redox reactions and the polarization curves of Sn and Se were studied to fix the pH and potential values V (NHE) to get uniform deposition. Films were cathodically deposited at 55°C. XRD studies show an orthorhombic structure. Films showed an indirect band-gap of 1.05 eV. Surface morphological studies were carried out using SEM, and the stoichiometry was estimated from XPS analysis. Effect of annealing in air at 200°C has been reported.

Keywords: Electrodeposition; Tin selenide; XRD studies; Optical band gap

1. Introduction

In search of new semiconducting materials for efficient solar energy conversion through photoelectrochemical solar cells, metal chalcogenides with layered structure are increasingly studied. These materials possess the following criteria to make them potential candidates in photoelectrochemical solar cells: (i) the band gap is between 1.0 and 2.0 eV, making them capable of absorbing a major portion of solar energy; (ii) they are chemically and electrochemically stable in either acid or alkaline condition; (iii) the constituent elements are abundantly available and cheap. Among the many chalcogenides IV–VI semiconductors, SnS, SnSe, GeS and GeSe meet these conditions closely, and are promising materials for energy conversion. These semiconductors form an interesting class of isomorphic materials, which are in many ways intermediate between two-dimensional systems and three-dimensional crystals.

Thin films of tin selenide (SnSe) are used in memory switching device [1]. Especially, SnSe belongs to the large class of layered semiconductor [2] with the SnSe layers stacked along the *c*-axis. It belongs to the space group Pmna (D_{2n}^{16}) which is deduced from a regular NaCl structure by different interionic spacing within the octahedral. It possesses a simple orthorhombic structure with constants: $a = 1.1157$, $b = 0.419$ and $c = 0.446$ nm. The unit cell contains eight atoms, placed in position by the scaled co-ordinates $\pm$ (u, 1/4, v) and $\pm$ (1/2 + u, 1/4, 1/2 − v), as in Fig. 1a [3]. The atoms are arranged in two adjacent double layers orthogonal to the largest cell dimensions as shown in Fig. 1b [4]. Within either double layer, each atom has three nearest neighbors and two next nearest neighbors. A sixth nearest neighboring atom lies in the other double layer and provides the bond between double layers. The resulting highly layered structure, typical of all orthorhombic chalcogenide crystals, causes a strong anisotropy of the physical properties of SnSe compounds [5]. Due to the anisotropy character, it is an attractive layered semiconductor compound and can be used as a cathodic material in lithium intercalation batteries.

SnSe has an energy gap of about 1.0 eV, which might prove as an efficient material for solar energy conversion [6]. However, no research has yet been conducted, to our knowledge, on the semiconducting and optical properties of electrodeposited SnSe thin films. In the present work, we show the electrical properties and optical absorption of SnSe films deposited onto tin oxide coated glass substrates.

2. Experimental

The deposition bath contains 50 mM of $SnCl_2$, 5 mM of SeO_2, and the pH of the solution was adjusted to 2.8 $\pm$ 0.1.

* Corresponding author. Fax:+91-4565-35202.
E-mail address: alagappa@md3.vsnl.net.in (C. Sanjeeviraja)

0040-6090/99/$ - see front matter
PII: S0040-6090(99)00644-6

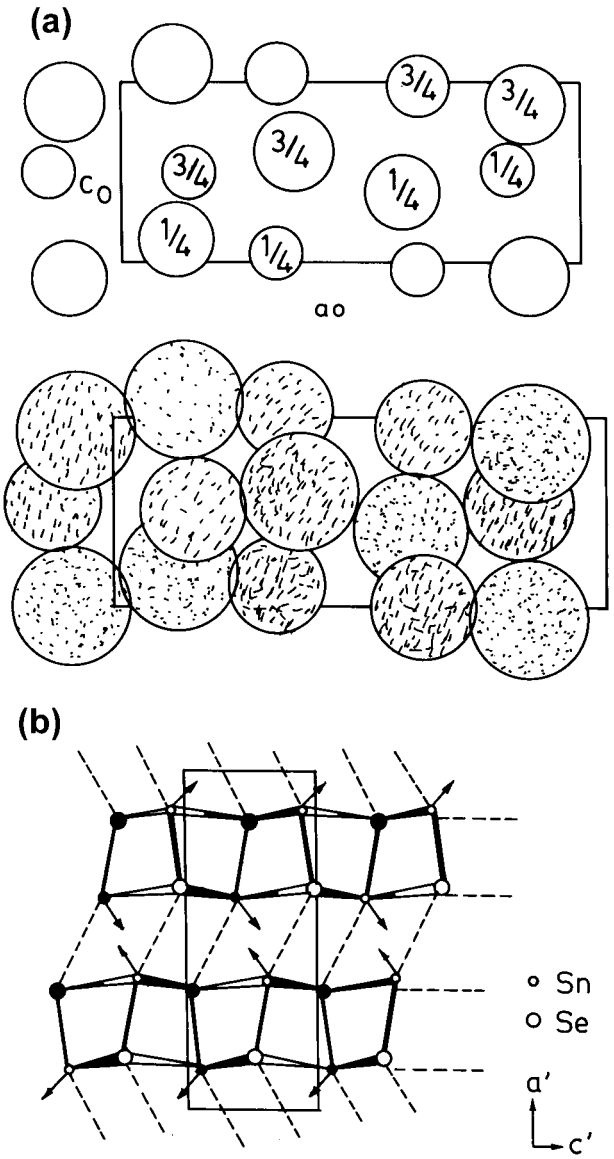

Fig. 1. Crystal structure of SnSe: (a) arrangement of atoms; (b) projection of atoms on *ac*-plane.

Films were deposited using a three electrode cells with water circulation and an EG&G-PAR model 362 scanning potentiostat/galvanostat. Tin oxide (TO)-coated glass substrates were rinsed well with deionized water and used as cathode for all studies. The deposition area was kept constant as 1 cm^2. A graphite electrode served as the anode. A saturated calomel electrode (SCE) was used as the reference electrode, and voltage values are expressed in NHE unless otherwise stated. Films were deposited by maintaining the bath temperature at 55°C. Annealing was performed in air at 200°C for 30 min. XRD studies were made using a JEOL JDX 803a X-ray diffractometer. The scanning electron microscopic (SEM) study was carried out using JSM 6400 JEOL Scanning Electron Microscope. The optical characterization of the films was carried out using a double beam Hitachi UV-vis-NIR U3400 spectrophotometer in the wave length region of 300–1500 nm. The X-ray photoelectron spectroscopy (XPS) spectrum was taken using VG Mkll ESCA spectrometer.

3. Results and discussion

3.1. Electrochemistry of Sn and Se

The inherent problem associated with the deposition of binary or ternary compounds is the widely varying individual deposition potential of the ions taking part in electrochemical reactions. If the individual potentials are much separated; to obtain co-deposition and stoichiometric compounds, one should bring their deposition potentials very close to both ions. The electrode potential for the deposition of selenium (Se) is more positive than that for tin (Sn). The individual electrochemical reaction steps involved in the deposition of Sn and Se are given as follows:

(i) Sn reduction: it involves a two electron transfer reaction

$$Sn^{2+} + 2e \rightleftharpoons Sn(s)$$

$$= E^0\left(Sn^{2+}/Sn\right) + (RT/2F)\ln a_{Sn^{2+}}/a_{Sn}$$

$$= -0.14V_{NHE} + 0.0295\log a_{Sn^{2+}}/a_{Sn}$$

(ii) Se reduction: selenous acid is formed on dissolving SeO_2 in water

$$SeO_2 + H_2O \rightleftharpoons H_2SeO_3$$

At pH 0–5, the steps, involving four electrons [7], associated with the reduction process to deposit Se are

$$H_2SeO_3 + 4H^+ + 4e^- \leftrightarrow Se(s) + 3H_2O$$

$$E^0(H_2SeO_3/Se) + (RT/4F)\ln\left(a_{HSeO_2^+}/a_{Se}\right) + (3RT/4F)\ln C_{H^+}$$

$$= 0.74V_{NHE} + 0.0148\log\left(a_{HSeO_2^+}/a_{Se}\right) - 0.0443pH$$

Here, E is the equilibrium electrode potential expressed with reference to NHE; 'a' is the activity of respective ions in the bulk solution and the deposit ($a = 1$, for an ion in the solid deposit); and C_H^+ is the concentration of hydrogen ions. Sn (s) and Se (s) are respective species in the solid deposit.

For simultaneous deposition of Sn and Se, the concentration and pH of the electrolyte should be adjusted so that the electrode potentials of the individual species come closer to each other. Tin is not corroded in moderately acidic, neutral and slightly alkaline solutions free from oxidizing agents, while it becomes corroded in very acidic and alkaline solutions [8]. Furthermore, some restrictions are imposed by the electrochemical reactions associated with selenium deposition. It is pH dependent and the deposition is favored when the bath pH is less than 5.0. Considering these competitive pH dependent electrochemical aspects of Sn and Se, the pH

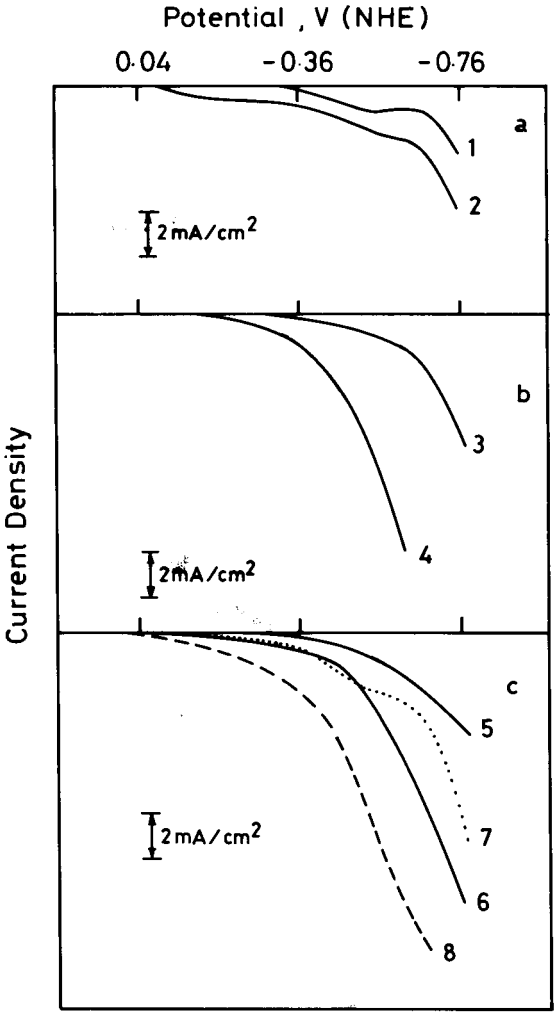

Fig. 2. Linear cathodic polarization curves of (a) Sn, (b) Se, and (c) theoretical curves for SnSe at room temperature (30°C) and 55°C.

of the bath is fixed between 2.0 and 3.5; deposition potential is fixed between −0.76 to +0.04 V (NHE). The pH of the fresh solutions used for deposition were about 2.0, which was increased to 2.8 by adding dilute ammonia solution. This pH was maintained throughout the deposition process.

3.2. Electrodeposition of Sn, Se and SnSe films

The concentrations of Sn and Se play a decisive role in obtaining co-deposited SnSe films and in the control of film stoichiometry. To achieve this, a very low ratio of Se (IV) to Sn (II) ions is recommended, and about 0.1 is found favorable to maintain the bath without any precipitation. It prevents fast depletion of ionic concentration in the bath. Another important aspect to be taken care of is the temperature dependence of the structural and electrical properties of the Se film. While amorphous and insulating Se films are deposited at room temperature, Se films with improved conductivity and crystalline nature are reported at 55°C and above [9]. Hence, the temperature of the bath was varied from room temperature to about 70°C and the cathodic polarization studies were conducted. A detailed study of the linear polarization curves of the deposition baths was performed with different concentration ratios of Sn and Se, and different bath temperatures. It shows that a relatively higher concentration of Sn(II) ions (50 mM) shift its deposition potential very close to that of Se(IV) ions (5 mM) while the bath temperature is maintained at 55°C.

The linear cathodic polarization curves of Sn and Se performed at room temperature (RT), 30°C, and at 55°C are shown in Fig. 2a,b, respectively. In Fig. 2a, curves 1 and 2 show the polarization curves of Sn at RT and 55°C. A positive shift in current flow is observed with increasing temperature, as is evident from the onset of current flow at −0.01 V and +0.09 V (NHE) at RT and 55°C, respectively. An overall current increase is seen throughout the polarization region, which shows that the reaction rate is enhanced at 55°C.

In Fig. 2b, curves 3 and 4 show the current-potential behavior of Se deposition at RT and 55°C. The current starts flowing at − 0.26 V at RT. A small passivity-like behaviour is observed at about −0.46 and then a sharp increase in reduction current is observed down to −0.76 V. At 55°C, the current flow starts at −0.01 V and a steep rise in current is observed, the maximum at −0.61 V. This may be attributed to the formation of moderately-conducting Se films at 55°C, compared to that of non-conducting films deposited at RT [9].

The experimentally observed linear polarization curves of the SnSe bath at RT and 55°C are compared with the theoretical curve as shown in Fig. 2c. The theoretical total current, involved in the process of SnSe formation, $I_{SnSe}(V)$, at each potential is calculated by adding the reduction currents of the individual species at the same potential. It is represented as

$$I_{SnSe}(V) = I_{Sn}(V) + I_{Se}(V)$$

assuming that, under the proposed experimental conditions, the reduction process of Sn does not interfere with that of Se. The experimental polarization curve of the bath containing both the Sn and Se species (curve 5) at RT shows overall lower current values compared to the theoretically calculated values (curve 7). A similar trend has been observed at 55°C, as observed from curves 6 and 8. This is due to the fact that under potential deposition of the noble element Se is taking place first, followed by Sn. Moreover, the selenium layer deposited, initially covers the conducting electrode surface, and subsequently makes a lesser conductive surface, over which the deposition of SnSe has to proceed. This type of resistive working electrode surface reduces the reaction rate, leading to a considerable decrease in the reduction current associated with the cathodic deposition of SnSe films. Based on these observations, a deposition potential of −0.56 V (NHE) was fixed for depositing SnSe films, which will prevent the interference of unwanted reduction processes, and hydrogen evolution, under the opti-

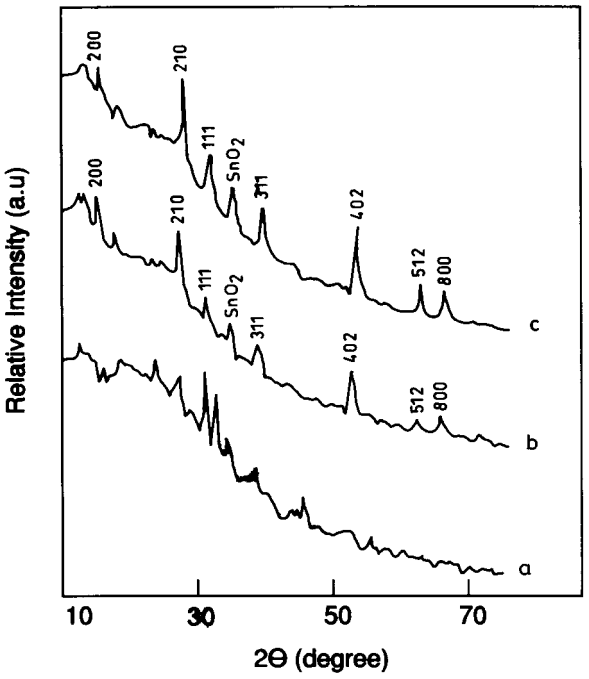

Fig. 3. X-ray diffraction pattern of (a) Sn, (b) SnSe thin films at bath temperature of 55°C, and (c) annealed at 200°C in air.

mized experimental conditions engaged in this study. Smooth, uniform, and well adherent films, were obtained with colors ranging from reddish-brown to gray.

3.3. Structural properties of SnSe films

The X-ray diffraction pattern shows the polycrystalline nature of the as- deposited films as shown in Fig. 3. For comparison, the XRD pattern of electrodeposited Sn films is given (Fig. 3a). XRD patterns of the electrodeposited SnSe film at 55°C (Fig. 3b), and annealed at 200°C for 30 min in air are shown (Fig. 3c). No Sn line is identified in the SnSe patterns. The observed *d*-values and the standard values are in good agreement, which confirms the deposition of stoichiometric SnSe films under the proposed optimized cathodic deposition conditions [10]. Annealing at

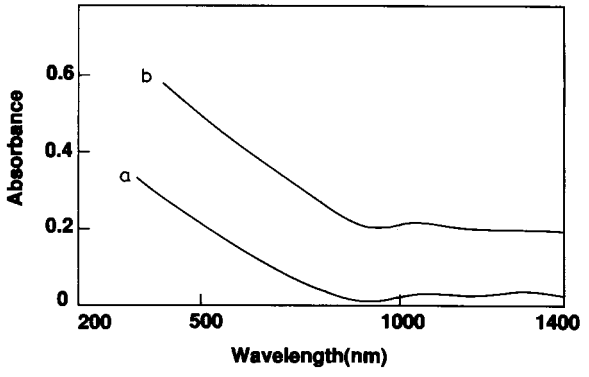

Fig. 4. Absorption spectra of the as-deposited SnSe thin film annealed at 200°C.

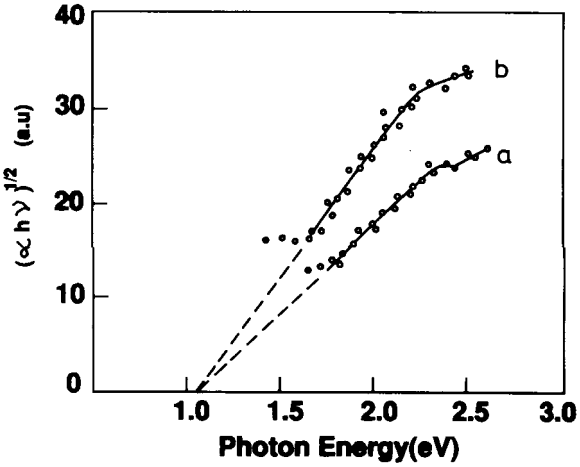

Fig. 5. A plot between $(\alpha h\nu)^{1/2}$ and $h\nu$ (eV) for SnSe thin film.

200°C improves the crystallinity and increases the grain size to about 5 μm. The films show an orthorhombic structure with lattice parameters: $a = 11.420$ Å, $b = 4.190$ Å and $c = 4.460$ Å. Both films show a preferential orientation along [210] and [402] directions. Using the hot-probe

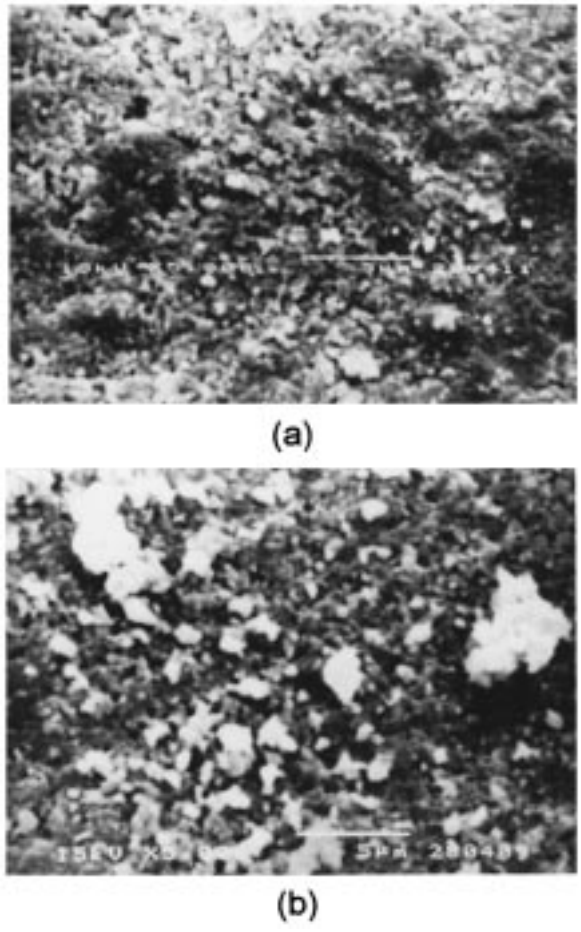

Fig. 6. SEM photograph of SnSe thin film: (a) as-deposited, and (b) annealed at 200°C.

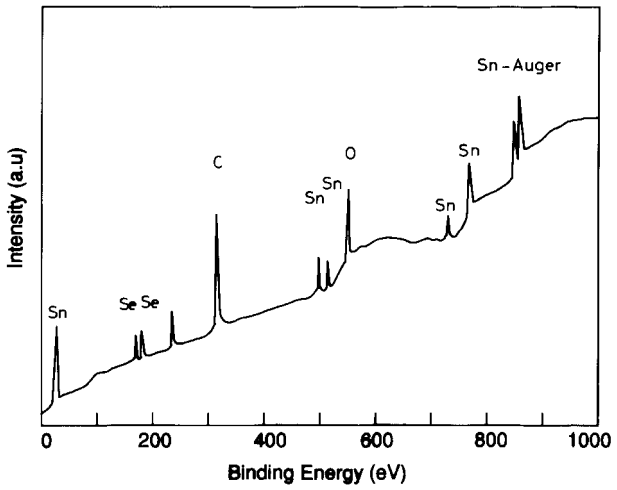

Fig. 7. Surface XPS spectrum of SnSe thin film.

method, it was observed that as-deposited and annealed films have p-type conductivity.

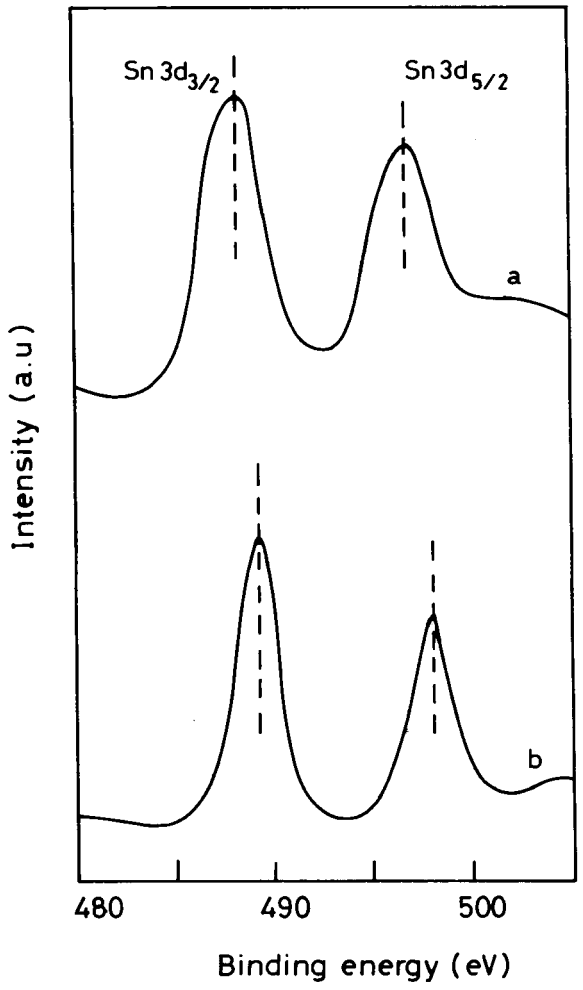

Fig. 8. High resolution scan of Sn 3d 3/2 and Sn 3d 5/2: (a) unetched top surface, and (b) sputtered inner surface.

3.4. Optical properties

The absorption behavior of the films was studied in the region of 300–1500 nm. Fig.4 shows the absorption spectra of the as-deposited film, and the films annealed at 200°C for 30 min in air. The films show good absorption in the visible region of 300–800 nm, and the annealing process increases the absorption behavior. A graph (Fig. 5) is plotted between $(\alpha h\nu)^{1/2}$ and $h\nu$ (eV). From the intercepts of the extrapolated linear region with the $h\nu$ axis, a band-gap value of 1.05 eV is observed for the as-deposited SnSe films, deposited at −0.56 V (NHE). It predicts that an indirect optical transition is associated with the electrodeposited SnSe films. It is in good agreement with the reported values for SnSe films [11] deposited by different techniques. The air annealed film has the same band-gap value of 1.05 eV. Engelken et al. [12] report an indirect band-gap of 0.95 eV for the as-deposited films.

3.5. SEM and XPS studies

Scanning electron microscope (SEM) studies were carried out to assess the quality of the SnSe films deposited at − 0.56 V (NHE). The surface morphology of the as-deposited films shows uniform grain size without pinholes, as seen in Fig. 6a. The grains are packed very closely and show a granular morphology. However, the films exhibited a hillock like surface. Annealing at 200°C for 30 min improved the surface smoothness, as is evident from Fig. 6b. The grain size also increases, leading to coalescence of the grains.

XPS spectrum (Fig. 7) confirms the presence of Sn and Se on the reddish-brown sample. However, the presence of O and C are also evident from the XPS analysis on different samples. Quantitative analysis of these elements shows a surface atomic concentration of 38.8% for Sn, 34.9% for Se, 12.5% for C and 13.8% for O. After 2 min sputtering, the atomic concentration changed to 47.4% for Sn and 43.1% for Se. Though there is an increase in the percent of Sn and Se at the inner surface compared to the top unetched surface, the ratio is almost the same at about 1:1. It shows that the films are nearly stoichiometric from top to bottom. The significant level of O may be due to an incipient corrosion process during preparation and handling. Fig. 8 shows XPS spectrum of the sample in the region of Sn 3d signal, in which Fig. 8a shows the Sn doublet of the top surface, and Fig. 8b shows the sputtered inner surface. The Sn 3d 5/2 (497.3 eV) and 3/2 (488.6eV) doublets were deconvulated into contribution from a low binding energy component due to Sn in SnSe. This is consistent with values reported for stoichiometric SnSe deposits.

4. Conclusion

The electrodeposition technique has been successfully used to obtain SnSe films from an aqueous solution contain-

ing stannous (Sn^{2+}) and selenite (SeO_3^{2-}) ions. A comparison of the linear polarization curves at RT and at 55°C, reveals some interesting information on the film formation processes. Deposition at 55°C favors the under potential formation of selenium which possesses more conductivity compared to the Se films deposited at RT. Stoichiometric SnSe films were deposited at a deposition potential of −0.56 V (NHE), keeping the bath pH at 2.8, and maintaining the bath temperature at 55°C. The as-deposited films are polycrystalline, and showed improved crystallinity and increased grain size on annealing at 200°C for 30 min. All the films showed p-type conductivity. The films have an orthorhombic structure with preferential orientation along [210] and [402] directions. Optical studies revealed the indirect nature of the films. They showed the same band-gap value of 1.05 eV, for both as-deposited and annealed films. However, annealing at 200°C increases the absorption behaviour of the films. The XPS spectrum of SnSe film shows the characteristic Sn(3d) doublet and Se(3p). Quantitative elemental analysis shows the presence of Sn and Se in a stoichiometric ratio of about 1:1, throughout the cross section of the film.

References

[1] T.S. Rao, B.K.S. Ray, A.K. Chaudhuri, Thin Solid Films 165 (1988) 257.
[2] G. Valicckonis, F.M. Gashimzade, D.A. Guscinova, G. Krivaite, M.M. Mamedev, A. Sileika, Phys. Stat. Sol. 122(b) (1984) 163.
[3] R.W.G. Wycoff, Crystal Structure, I, Wiley, New York, 1963.
[4] P.S. Del Bucchia, J.C. Jumas, M. Maurin, Acta Cryst. B37 (1981) 1903.
[5] R.K. Bedi, Conference on the Physics and Technology of Semiconductor Devices and Integrated Circuits; 5–7 Feb., IIT Madras, India, 1992, p. 104
[6] D.T. Quan, Thin Solid Films 149 (1987) 197.
[7] G. Jarzabek, Z. Kublik, J. Electroanal. Chem. 114 (1980) 165.
[8] M. Pourbaix, Atlas of Electrochemical Equilibria in Aqueous Solutions, National Association of Corrosion Engineers, Houston TX, 1974.
[9] S. Cattarin, F. Faurlanetto, M.M. Musiani, J. Electroanal. Chem. 415 (1996) 123.
[10] J.P. Singh, R.K. Bedi, J. Appl. Phys. 68 (1990) 2776.
[11] S. Maheshwar, P. Veluchamy, C. Natarajan, D. Kumar, Electrochim. Acta 36 (1991) 1107.
[12] R.D. Engelken, A.K. Berry, T.P. van Doron, J.L. Boone, A. Sohnazary, J. Electrochem. Soc. 133 (1986) 861.